

1 **An integrative approach to investigate natural variation  
2 in the accumulation of aliphatic glucosinolates in  
3 *Arabidopsis thaliana***

4 Suraj Sharma<sup>1,2</sup>, Ovidiu Popa<sup>2</sup>, Stanislav Kopriva<sup>1,3</sup>, Oliver Ebenhoeh<sup>1,2</sup>

5 <sup>1</sup> Cluster of Excellence on Plant Sciences (CEPLAS), Heinrich-Heine University Duesseldorf,  
6 Germany

7 <sup>2</sup> Institute for Theoretical Biology, Heinrich-Heine University Duesseldorf, Germany

8 <sup>3</sup> Botanical Institute, University of Cologne, Germany

9

10 **Abstract**

11 Glucosinolates are a fascinating class of specialised metabolites found in the plants of  
12 *Brassicaceae* family. The variation in glucosinolate composition across different *Arabidopsis*  
13 ecotypes could be a result of allelic compositions at different biosynthetic loci. The  
14 contribution of methylthioalkylmalate synthase (MAM) genes to diversity of glucosinolate  
15 profiles across different *Arabidopsis* ecotypes has been confirmed by genetic analyses.  
16 Different MAM isoforms utilise different chain-elongated substrates for glucosinolate  
17 biosynthesis causing thus a variation in chain lengths across different *Arabidopsis* ecotypes.  
18 To further investigate the relationship between the genotype and the associated metabolic  
19 phenotype, we studied the diversity of genes and enzymes of glucosinolate biosynthesis.  
20 Using Shannon entropy as a measure we revealed that several genes of the pathway show a  
21 clear derivation from the expected behaviour, either accumulating non-synonymous SNPs or  
22 showing signs of purifying selection. We found that the genotype-phenotype relationship is  
23 much more complicated than inferred from the diversity of MAM synthases. We conclude  
24 therefore, that the ON/OFF feature of key QTLs is not enough to elucidate the diversity of  
25 glucosinolates across different *Arabidopsis thaliana* ecotypes and that glucosinolate profiles  
26 are determined also through the polymorphic residues along the coding regions of multiple  
27 metabolic genes.

## 28 Introduction

29 Plant secondary metabolism produces a huge variation in structures and molecules with a  
30 plethora of functions for the plants but also for human nutrition and health (Owen, Patron,  
31 Huang, & Osbourn, 2017). One class of such secondary metabolites are glucosinolates in the  
32 Brassicaceae. Glucosinolates (GSLs) are important for the plants as a defence against  
33 herbivores, fungi, and other pathogens (Halkier & Gershenzon, 2006). They are also  
34 determinants of taste and flavour of cruciferous vegetables and responsible for their positive  
35 health properties (Traka & Mithen, 2009). More than 140 different GSL structures have been  
36 described, with a great variation not only between species, but also among ecotypes of the  
37 same species (Agerbirk et al., 2015; Clarke, 2010). GSLs are synthesised from amino acids  
38 and are divided into three classes: aliphatic GSLs, derived from alanine, leucine, isoleucine,  
39 valine and methionine (Met), indolic GSLs synthesised from tryptophan, and aromatic GSLs  
40 from phenylalanine (Phe) (Halkier & Gershenzon, 2006; Sønderby, Geu-Flores, & Halkier,  
41 2010). All GSLs possess the same core structure, which comprises a glucose residue linked to  
42 a (Z)-N-hydroximic sulfate ester via a sulphur atom (Fahey, Zalcman, & Talalay, 2001).  
43 GSL biosynthesis consists of three independent steps: (i) chain elongation of selected  
44 precursor amino acids (only Met and Phe), (ii) formation of the core GSL structure, and (iii)  
45 secondary modifications of the amino acid side chain. The diversity of GSLs derives from the  
46 side-chain elongation and secondary modifications.

47 GSLs are best known for their function in interaction between plants and herbivores.  
48 Upon tissue damage, the GSLs stored in the vacuoles come in contact with the enzyme  
49 myrosinase, which cleaves the thio-glucoside bond. The resulting aglycones are unstable and  
50 form volatile isothiocyanates or nitriles (Halkier & Gershenzon, 2006). Depending upon the  
51 herbivore, the volatiles of specific GSLs can act as feeding deterrents or stimulants (Buskov,  
52 Serra, Rosa, Sørensen, & Sørensen, 2002; Gabrys & Tjallingii, 2002; Lazzeri, Curto, Leoni,  
53 & Dallavalle, 2004; Mewis, Ulrich, & Schnitzler, 2002; Miles, Campo, & Renwick, 2005;  
54 Noret et al., 2005). Therefore, there is often an overlap between quantitative trait loci (QTL)  
55 for GSL accumulation and insect resistance (Kroymann, Donnerhacke, Schnabelrauch, &  
56 Mitchell-Olds, 2003). A possible outcome of this heterogeneous natural selection on GSLs is  
57 the quick evolution of new compounds or new patterns of compound accumulation  
58 (Daxenbichler et al., 1991; Rodman, 1980). New GSLs may increase resistance to herbivores  
59 that have become adapted to existing defences, whereas new patterns of GSL accumulation

60 may provide a unique complement of defences by slowing down the counter-adaptation of  
61 herbivores.

62 The GSL defence system is one of the few systems where systematic data assessing  
63 between and within species variation at both phenotypic and causal genetic level is available  
64 (Halkier & Gershenzon, 2006; Sønderby et al., 2010). Natural variation within or between  
65 species is regulated by a complex network of genes and associated polymorphisms (Fisher,  
66 1930; Kliebenstein, Kroymann, et al., 2001; Lynch, Walsh, & others, 1998). These variations,  
67 however, complicate our understanding of how certain genes behave in context of a species  
68 as we often study a single genotype. Thus, understanding a metabolic pathway requires  
69 studies involving more than one ecotype. For example, methionine derived aliphatic GSLs  
70 differ in length of the side chain caused by the elongation of the amino acid, as well as by  
71 further modifications, e.g. oxidation of the sulfur atom (Halkier & Gershenzon, 2006;  
72 Sønderby et al., 2010). In the model plant *Arabidopsis thaliana*, aliphatic GSLs of six  
73 different chain-lengths, referred to as 3C to 8C GSLs, but with different side chains are  
74 found. The diversity in length of aliphatic GSLs can be explained by the variation in the  
75 iterative chain-elongation cycles, each adding one methylene group to the Met and/or  
76 elongated Met molecule (Halkier & Gershenzon, 2006). The QTL responsible for  
77 determining the chain-elongation of GSLs is GS-ELONG (Magrath et al., 1994). GS-ELONG  
78 is highly variable across different *Arabidopsis* ecotypes, with common large indel  
79 polymorphism (Kroymann et al., 2003). The gene underlying the GS-ELONG QTL is  
80 methylthioalkylmalate synthase (MAM3), encoding the key enzyme of the chain elongation  
81 cycle (Kroymann et al., 2001). However, the GS-ELONG locus harbours two more genes,  
82 isoforms of MAM3 called MAM1 and MAM2. MAM3 is present in all *Arabidopsis* ecotypes,  
83 and some ecotypes possess both additional genes whereas others possess either MAM1 or  
84 MAM2, with some, such as *Landsberg erecta* (*Ler*), having a truncated (non-functional)  
85 MAM1 in addition to MAM2 (Kroymann et al., 2003). While the presence of functional  
86 MAM genes has been described as responsible for the variation in aliphatic GSL side chain  
87 length, very little is known about contribution of other genetic variation, mainly single  
88 nucleotide polymorphism (SNP), at this locus.

89 In this paper, we investigate the link between the diversity of GSL enzyme-coding  
90 genes and their GSL profiles exhibited across 72 different *A. thaliana* ecotypes. The selection  
91 of 72 ecotypes is based on the availability of information about the gene sequences and the  
92 patterns of accumulation of aliphatic glucosinolates. Importantly, the experiments for

93 determining the aliphatic glucosinolate levels have been performed under identical conditions  
94 (Chan, Rowe, & Kliebenstein, 2010; Kliebenstein, Kroymann, et al., 2001). It can therefore  
95 be assumed that the environment was identical (up to experimental precision) for all  
96 ecotypes. This study presents an effort to quantify the impact of the diversity of MAM gene  
97 sequence on GSL variation, rather than the on/off nature of the GS ELONG QTLs. The  
98 genetic sequence coding for an enzyme determines the kinetic properties of the corresponding  
99 enzyme. For example, polymorphisms in the active sites, in principle, can change the  
100 substrate specificity of the respective enzyme. Thus, we investigate the level of  
101 polymorphisms in the coding region of the GSL enzymes to study the impact on the diversity  
102 of aliphatic GSLs.

103 **Results**

104 **Distribution of MAM genes across *Arabidopsis thaliana* ecotypes**

105 The genetic basis of chain-length distribution of aliphatic GSLs became evident with the  
106 identification of the GS-ELONG QTL in *Arabidopsis* and *Brassica napus* (Magrath et al.,  
107 1994). The locus was mapped in *Arabidopsis* by using a cross between two ecotypes,  
108 *Columbia (Col)* and *Landsberg erecta (Ler)*, where the major glucosinolates are 4C and 3C,  
109 respectively (Kroymann et al., 2001). The underlying candidates *MAM1* and *MAM3* genes are  
110 two adjacent sequences with high similarity to genes encoding isopropylmalate synthase that  
111 catalyses the condensation of chain elongation in leucine biosynthesis. Later, a third MAM-  
112 like gene, *MAM2*, was identified at the same locus as *MAM1* (Kroymann et al., 2003). While  
113 *MAM3* is ubiquitous, most *Arabidopsis* ecotypes examined possessed functional copies of  
114 either *MAM1* or *MAM2* genes. A functional *MAM1* gene has been correlated with the  
115 accumulation of 4C GSLs, whereas a functional *MAM2* has been linked to 3C GSLs. To gain  
116 more insights on the impact of MAM synthases on chain lengths distribution of aliphatic  
117 GSL, we analysed the similarity of the annotated *MAM1* gene across 72 *Arabidopsis* ecotypes  
118 taken from 1001 genome project database (Jorge et al., 2016). These ecotypes were selected  
119 based on the availability of gene sequences and the associated aliphatic GSL profiles. Details  
120 on the 72 ecotypes are given in the Supplementary Table 1. The annotated *MAM1* sequences  
121 from the 72 ecotypes were compared to each other for diversity. Figure 1 shows a mid-point  
122 rooted phylogenetic tree showing the evolutionary relationship between the ecotypes based  
123 on the similarities and differences in the coding region of the *MAM1/MAM2* sequences.  
124 Based on maximum likelihood estimation (Guindon et al., 2010), the tree shows two main

125 branches. While 53 out of the 72 ecotypes clustering in the blue branch indeed possess high  
126 similarity to the coding region of *MAMI* gene, 19 ecotypes in the red branch possess genes  
127 more like the *MAM2* gene. Thus, we assume that the ecotypes composed in blue and red  
128 branches possess *MAMI* and *MAM2* genes, respectively.

129 The metabolic genotypes and associated phenotypes

130 We define a metabolic genotype ( $G_i$ ) as the gene sequence of enzymes of glucosinolate  
131 biosynthesis in ecotype  $i$ , whereas the metabolic phenotype ( $P_i$ ) corresponds to the  
132 composition of aliphatic GSLs in the ecotype  $i$ . To gain a deeper understanding of how  
133 different metabolic genotypes and their associated phenotypes are linked, we analysed the  
134 genotypic and phenotypic distances. The genotypic distances between the genotypes were  
135 calculated as Hamming distance (Hamming, 1950)  $d_{i,j}^G$ , which is the number of positions at  
136 which the corresponding nucleotide/amino-acid characters are different between gene  
137 sequences  $G_i$  and  $G_j$  of equal length. The phenotypic distance  $d_{i,j}^P$  was calculated as  
138 Euclidean distance,  $d_{i,j}^P = \sqrt{\sum_{k=1}^n (P_{i,k} - P_{j,k})^2}$  between two phenotypes  $P_{i,k} =$   
139  $(P_{i,1}, P_{i,2}, \dots, P_{i,n})$  and  $P_{j,k} = (P_{j,1}, P_{j,2}, \dots, P_{j,n})$  in an  $n$ -dimensional space. In this study,  
140  $n=6$ , which corresponds to the total number of chain-elongated aliphatic GSLs found in *A.*  
141 *thaliana* (Figure 2). Thus, we can quantify differences between all pairs of ecotypes based on  
142 their metabolic genotype  $G_i$  ( $i = 1, \dots, 72$ ) and phenotype  $P_i$  ( $i = 1, \dots, 72$ ). Figure 3  
143 showcases the summary of the analysis, where the genotypic distances are plotted against the  
144 phenotypic distances. Intuitively, one would assume that similar genotypes shall exhibit  
145 similar phenotypes, and *vice-versa*. However, Figure 3 clearly shows that several ecotypes  
146 show low genotypic distance (i.e. they are genotypically similar) but exhibit high phenotypic  
147 distance (variation in GSL profiles). Also, there exist genotypically diverse ecotypes that  
148 exhibit very similar GSL profiles. Thus, investigating the factors affecting variations in the  
149 phenotypes of such ecotypes will provide a clearer understanding of how distinct patterns of  
150 GSL accumulation emerge out of genetic differences. Moreover, investigation of the  
151 localisation of polymorphic residues in the GSL biosynthesis enzymes will provide a better  
152 understanding of the link between metabolic genotype and the associated metabolic  
153 phenotypes.

154 Diversity of GSL enzyme-coding genes

155 To investigate the diversity of metabolic genes of GSL biosynthesis, we investigated the  
156 levels of amino acid and nucleotide polymorphism across the 72 *A. thaliana* ecotypes by  
157 calculating the average Shannon entropy (Shannon)  $H$  across the gene length (Figure 4A and  
158 B). The analysis revealed that some of these enzymes are highly diverse while others remain  
159 conserved across different ecotypes. Interestingly, the diversity seems to be independent of  
160 steps of GSL biosynthesis in which the enzymes are active. From the diversity of amino acid  
161 sequences (Figure 4A), *FMO-GSOX1* enzyme exhibits the highest diversity (entropy), while  
162 the lowest diversity is found in *SOT17*. Among the enzymes active in the chain-elongation  
163 pathway, *MAMI* shows the highest diversity while *BAT5* shows the low diversity. However, a  
164 further analysis of the diversity in the nucleotide sequences of the metabolic genotypes  
165 showed a high level of polymorphism in *BAT5* (cf. Figure 4B), which was not reflected in  
166 the diversity of amino acid sequences. Indeed, most genes show only a slightly lower  
167 diversity in amino acid variation than nucleotide variation, which reflects the degeneration of  
168 the genetic code (Figure 4C). A plausible explanation for the low amino acid variation in  
169 *BAT5* could be the specificity towards a variety of chain-elongated substrates of GSL  
170 biosynthesis (Halkier & Gershenson, 2006). The low diversity of *BAT5* could be linked to its  
171 function in transport of a diverse range of compounds that are a part of aliphatic GSL  
172 biosynthesis and Met-salvage pathway (Gigolashvili et al., 2009; Sauter, Moffatt, Saechao,  
173 Hell, & Wirtz, 2013), thus, mutations in the coding region of *BAT5* may impair the  
174 functioning of both pathways. In contrast to *BAT5*, *FMO-GSOX1* shows a low diversity in the  
175 nucleotide sequences of 72 genotypes but reflect a high diversity in the amino acid  
176 sequences. This is a clear example of preferential accumulation of non-synonymous  
177 mutations, which alter the amino acid sequence of an enzyme.

178 High diversity of *MAMI* could be a consequence of incorrect annotation of *MAMI/MAM2*  
179 enzymes across 72 *A. thaliana* ecotypes. Thus, we analysed the diversity of GSL enzymes  
180 across the *MAM1* ecotypes (blue branch of Figure 1) and *MAM2* (red branch of Figure 1)  
181 ecotypes, separately. We did see a reduction in the diversity of *MAM1* and *MAM2* enzymes  
182 (cf. Supplementary Figure 1 and Supplementary Figure 2). Nevertheless, *MAMI* and *MAM2*  
183 are still the most diverse enzymes of chain-elongation pathway.

184 Polymorphisms in the active sites of MAM enzymes

185 To get a clearer understanding of the effects of the localisation of polymorphic amino acid  
186 residues in the active sites of the metabolic enzymes, we extracted the information about the

187 active sites from the NCBI's conserved domain database (Marchler-Bauer et al., 2015). For  
188 example, the amino acid positions 93, 94, 97, 124, 162, 164, 186, 227, 229, 231, 257, 259,  
189 260, 261, 262, 290, 292, and 294 are known to be key for activity of MAM synthases, based  
190 on the database and a crystal structure (Kumar et al., 2019; Marchler-Bauer et al., 2015;  
191 Petersen et al., 2019). We refer to the amino acid positions from 93 to 294 as active region of  
192 the enzyme. We have found that MAM synthases exhibit a maximum of 13 and 3  
193 polymorphic residues in the active region of MAM1 and MAM3, respectively. Figure 5(A)  
194 and (B) show pairwise comparisons of polymorphisms in the active region of MAM  
195 synthases against the genotypic distances of 72 *A. thaliana* ecotypes. Furthermore, we  
196 recorded the polymorphisms at different positions in the active region of MAM synthases  
197 (see Figure 5(C)). The amino acid residues at position 98, 99, 132, 138, 139, 147, 165, 173,  
198 177, 187, 228, 245, 257, 258, 271, 289 and 290 of the *MAM1* and positions 156, 231, 241 and  
199 242 of *MAM3* accumulate polymorphic residues across the 72 *Arabidopsis* ecotypes.  
200 Polymorphisms in the active sites of an enzyme, in principle, can change the catalytic  
201 properties of the enzyme (Kroymann et al., 2001; Kumar et al., 2019; Petersen et al., 2019).  
202 However, the quantitative effect on the enzymatic properties cannot be explained due to  
203 unavailability of enzyme abundances in these 72 ecotypes.

## 204 Discussion

### 205 Plasticity of the metabolic genotype and the associated GSL profiles

206 Glucosinolate metabolism results in a highly variable composition of individual metabolites  
207 in *Arabidopsis* accessions, which is reflected by a corresponding high diversity at the causal  
208 genetic level. Thus, it serves as a suitable model system to investigate the broader aspects of  
209 genotype-phenotype relationships. Allelic composition at several glucosinolate biosynthetic  
210 loci drive different glucosinolate profiles among *A. thaliana* ecotypes (Kliebenstein,  
211 Kroymann, et al., 2001). These variations, however, are often in the form of presence and/or  
212 expression of one or other copy of a duplicated gene, such as the *AOP2* and *AOP3* at the GS-  
213 ALK/GS-OHP locus (Kliebenstein, Lambrix, Reichelt, Gershenzon, & Mitchell-Olds, 2001),  
214 or the *MAM1/MAM2* at GS-ELONG (Kroymann et al., 2003), which complicates our  
215 understanding of how genetic variations lead to metabolic properties of the enzymes encoded  
216 by the respective genes. The Met-derived aliphatic GSLs are the most abundant form of  
217 glucosinolates in *A. thaliana* and many *Brassicaceae* crops (Agerbirk & Olsen, 2012;  
218 Benderoth et al., 2006; Halkier & Gershenzon, 2006; Kliebenstein, Kroymann, et al., 2001;

219 Kroymann et al., 2003; Textor et al., 2004; Textor, de Kraker, Hause, Gershenzon, &  
220 Tokuhisa, 2007). The chain-elongation pathway of GSL biosynthesis is crucial for generating  
221 the chain-length diversity of aliphatic GSLs and for connecting primary and specialised  
222 metabolism. Although the evolution of core features of aliphatic GSL biosynthesis in  
223 *Arabidopsis* has been studied (He et al., 2011; Sawada et al., 2009; Textor et al., 2004;  
224 Wittstock et al., 2004), the molecular basis for diversity of function of MAM synthases and  
225 the role of different MAM isoforms within *A. thaliana* accessions is not sufficiently  
226 understood. The chain-length distribution of different aliphatic GSLs has so far been  
227 attributed to the presence of different MAM isoforms, namely *MAMI*, *MAM2* and *MAM3*  
228 (Halkier & Gershenzon, 2006; Kroymann et al., 2003; Textor et al., 2004, 2007). By  
229 investigating the differences in sequences of MAM synthases across *A. thaliana* ecotypes, we  
230 show that the ecotypes can be broadly classified in two groups based on the similarity to  
231 either of *MAMI* and *MAM2* genes as also expected from the genomic composition of the  
232 *GS\_ELONG* locus (cf. Figure 1). Correspondingly, the GSL profiles from different ecotypes  
233 can be broadly classified into two major groups based on the phenotypic distance  $d_{i,j}^P$   
234 between different GSL profiles (cf. Figure 2). However, the groups classified based on either  
235 of phenotypic distances or the similarity of MAM synthases are not identical. This points to a  
236 more complicated relationship between the genotype and the associated GSL profiles. Thus,  
237 estimating the pattern of GSL accumulation based solely on the distinction between *MAM1*  
238 and *MAM2* enzymes is not feasible.

### 239 Diversity of genes beyond classical QTLs

240 The heterogeneity in the genetic makeup of the metabolic genes across different *A. thaliana*  
241 ecotypes and their associated metabolic phenotypes are an excellent tool for investigating the  
242 mechanisms of adaptation and functional diversification (Mitchell-Olds & Schmitt, 2006;  
243 Pigliucci, 2010). Comparing the diversity of genes of GSLs synthesis we expected to find the  
244 highest diversity in genes of the chain-elongation and secondary modification, because these  
245 steps contribute highly to the diversity of the GSLs. However, surprisingly, we found that the  
246 level of diversity appears to be unrelated with the functional role of the gene within the GSL  
247 metabolic pathway (cf. Figure 4). While as expected, the least diverse enzyme was SOT17,  
248 part of the core synthesis, another enzyme of the core pathway, SUR1, was the fourth most  
249 diverse from 30 enzymes (Figure 4). This is surprising, since loss of enzymes of the core  
250 synthesis, such as *UGT74B1* or *SUR1* has a much higher impact on the total GSLs than loss  
251 of enzymes of the side chain modification (Douglas Grubb et al., 2004; Keurentjes et al.,

252 2006; Mikkelsen, Naur, & Halkier, 2004). Thus, it seems that enzymes of all parts of GSL  
253 biosynthesis can contribute to the diversity of the metabolites. Surprisingly, while  
254 investigating the second least diverse enzyme *BAT5*, part of chain-elongation of aliphatic  
255 GSLs, we found that it is highly diverse in the nucleotide sequence (see Figure 4B). It can be  
256 a consequence of purifying natural selection that prevents the change of an amino acid  
257 residue at a given position in a multiple alignment, thus favouring an excess of synonymous  
258 versus non-synonymous substitutions. It is much more difficult, however, to explain the  
259 results of *FMO-GSOX1*, which shows a large variation in amino acid sequence derived from  
260 a relatively low variation in DNA sequence. Nevertheless, it is evident that *FMO-GSOX1*  
261 favours non-synonymous substitutions versus the synonymous substitutions, possibly linked  
262 to the function in the secondary modification of glucosinolates, responsible for large part of  
263 the structural variation. Multiple genetic analyses revealed that, in general, few key QTLs  
264 shape the metabolic phenotype. In contrast, our analysis detected diversity of the metabolic  
265 genes across the whole pathway, irrespective of their association to a major QTL. However,  
266 how far this variation in gene/protein sequence contributes to the phenotypic variation  
267 remains to be elucidated.

268 The genotype-phenotype relationship

269 Nowhere is the contribution of subtle sequence diversity to variation in GSLs more apparent,  
270 than in the MAM genes. In *A. thaliana*, the enzyme isoforms *MAM1* and *MAM2* catalyse the  
271 formation of short-chain (3C and 4C) aliphatic GSLs, whereas the isoform *MAM3* catalyses  
272 the formation of both short-chain and long-chain (5C-8C) GSLs (Halkier 2006). Indeed,  
273 orthologues of *MAM1* and *MAM2* are also responsible for diversity of aliphatic GSLs across a  
274 range of *Brassica* species (Kumar et al., 2019). The distinct function of the two genes was  
275 confirmed by complementation of Arabidopsis *mam1* mutant, when *MAM1* from *B. juncea*  
276 restored wild type GSL profile but *MAM2* did not (Kumar et al., 2019). Our investigation of  
277 genotypic and phenotypic distances between different Arabidopsis ecotypes showed that  
278 some ecotypes have identical metabolic genotype but exhibit high diversity in their associated  
279 metabolic phenotype, and *vice-versa* (cf. Figure 3). Therefore, the relationship between the  
280 metabolic genotypes and the phenotypes are much more complicated than a link to one of the  
281 *MAM1/MAM2* gene pair. Indeed, the role of individual amino acid alterations between these  
282 two genes demonstrates clearly that also SNPs can have a great effect on the phenotypes.  
283 Thus, mutagenesis of serine to phenylalanine at position 102 and alanine to threonine at 290,  
284 parts of active region of *MAM1* changed the distribution of C3 to C4 GSLs (Kroymann et al.,

285 2001) in *A. thaliana*. Alterations in four other amino acids in *B. juncea* MAM1 affected the  
286 kinetic properties of the enzyme to more MAM2-like and *vice versa* (Kumar et al., 2019).  
287 Also, in Arabidopsis MAM1 alteration of further three amino acids resulted in changes of the  
288 pattern of elongation products *in vitro* (Petersen et al., 2019). To further investigate the  
289 impact of MAM synthases on chain-length distribution of aliphatic GSLs, we analysed the  
290 polymorphisms in the active region of MAM synthases. From our analysis of the diversity of  
291 the active region of MAM synthases, we conclude that *MAM1* is highly variable across its  
292 active region and accumulate up to 13 polymorphic amino-acid residues at 17 different  
293 locations in the active region. Whereas, the active region of *MAM3* is comparatively  
294 conserved and only accumulates a maximum of 4 polymorphic residues at 3 locations in the  
295 active region, naturally (cf. Figure 5). It is known that polymorphisms in active site of MAM  
296 synthases change the specificity of a metabolic enzyme towards respective substrates of  
297 aliphatic GSL biosynthesis (Kumar et al., 2019; Petersen et al., 2019). This results in  
298 different composition and the total accumulation of aliphatic GSLs across different  
299 *Brassicaceae* species, including *Arabidopsis thaliana* (Kroymann et al., 2001; Kumar et al.,  
300 2019; Petersen et al., 2019). The above analysis, however, only showcases one of the two  
301 possibilities by which a genotype can exhibit a metabolic phenotype. The gene regulatory  
302 networks can also change the expression of metabolic genes, which in turn changes the  
303 enzyme abundance and thus results in different metabolic phenotypes (de Kraker &  
304 Gershenzon, 2011; Kumar et al., 2019; Petersen et al., 2019). Although, numerous studies  
305 have shown that a multitude of genes and underlying regulatory processes are involved in the  
306 diversity of specialised metabolites such as glucosinolates (Chan et al., 2010; Koornneef,  
307 Alonso-Blanco, & Vreugdenhil, 2004; Kumar et al., 2019; LASKY et al., 2012; Petersen et  
308 al., 2019), interpreting the findings in the context of metabolic properties is highly  
309 challenging. This is particularly due to a missing stringent definition of the genotype–  
310 phenotype relationship, which can hardly be expected to be derivable from a single  
311 methodology but rather requires a comprehensive platform of combined experimental and  
312 theoretical strategies (DIZ, MARTÍNEZ-FERNÁNDEZ, & ROLÁN-ALVAREZ, 2012;  
313 Sharma, 2018; Weckwerth, Wenzel, & Fiehn, 2004).

## 314 Conclusion

315 Altogether we show here that the control over phenotypic diversity in glucosinolates is  
316 potentially spread over the whole pathway. On the example of MAM1 and MAM2,  
317 responsible for side chain elongation of Met-derived glucosinolates, we revealed that

318 sequence variation beyond the presence of one or the other isoform contributes to the  
319 variation in chain length. The present study thus points to the necessity to pay attention to  
320 variation beyond the classical ON/OFF features of key metabolic QTLs, for investigating the  
321 diversity of specialised metabolic pathways, such as glucosinolates. Since the recent efforts  
322 towards unravelling the genotype-phenotype relationships focus at either experimental  
323 studies with a selection of genotypes or computational approaches to correlate the observed  
324 experimental observations, it is crucial to develop frameworks that integrate multi-omics data  
325 with fundamental rules of metabolic modelling to fully understand how particular genotype is  
326 reflected in a phenotype.

## 327 Materials and Methods

### 328 Genotypic data

329 Information about the nucleotide and amino acid composition of 30 GSL biosynthesis genes  
330 from 72 *A. thaliana* ecotypes was taken from the 1001 genomes project (Jorge et al., 2016).  
331 The reason behind selecting these 72 ecotypes was the availability of Met-derived GSL  
332 composition under identical environmental conditions. To obtain the gene sequences of the  
333 ecotypes of interest, we used an inhouse R-script that converts the TAIR10 version of SNP  
334 (single nucleotide polymorphisms) files provided by the 1001 genome database into an R-  
335 object. This R-object is a sparse matrix containing the nucleotide information for each  
336 ecotype at each locus in the reference genome coded as numbers. Non-polymorphic sites are  
337 coded as 0, polymorphic ones as 1,2,3,4 or 5 depending if at the specific locus an A, C, G, T  
338 or indel was observed. From this R-Object we could extract the nucleotide sequences of a  
339 specific ecotype for each coding region of interest. To obtain the amino acid sequence we  
340 used the function '*translate*' from the R-package 'seqinr'.

### 341 Phenotypic data

342 Experimental data of Met-GSLs concentrations were obtained from Chan et al. (2010) and  
343 Kliebenstein et al. (2001). The final set of GSL data is given in Table 1. The data is  
344 composed of normalised concentrations of six aliphatic GSLs, referred to as 3C to 8C, from  
345 72 different ecotypes of *A. thaliana* under controlled and identical experimental conditions.

346

### 347 Calculation of diversity using Shannon entropy

348 The nucleotide/amino-acid composition of the coding regions of GSL genes from 72 *A.*  
349 *thaliana* ecotypes is described as a set of relative probability,  $p_{i,j}$ , for the  $i^{th}$  nucleotide/amino-  
350 acid ( $i = 1, 2, \dots, n$ ) in the  $j^{th}$  ecotype ( $j = 1, 2, \dots, 72$ ). Then, the diversity of each position  
351 in the coding region can be quantified by Shannon entropy (Shannon, 1948),

$$H_i = - \sum_j^n p_{i,j} \log p_{i,j}$$

352  $H_i$  will vary from zero, when the  $i^{th}$  nucleotide/amino-acid is same across all 72 ecotypes, to 1  
353 when the probability is equal for observing all nucleotides/amino-acids at same locus across  
354 72 ecotypes. Moreover, to get an estimate of diversity of a nucleotide/amino-acid sequence of  
355 length  $n$ , we calculate the average entropy  $H^{avg}$  as

$$H^{avg} = \frac{1}{n} \sum_i^n H_i$$

### 356 Phylogenetic tree reconstruction

357 Amino acid sequences of the MAM loci from the 72 ecotypes were aligned using 'mafft' ver.  
358 v7.407 (Katoh & Standley, 2013) with the parameter '--maxiterate 1000 --globalpair --  
359 phylipout' to obtain a multiple sequences alignment in phylip format. This was then used as  
360 input for phym (20120412) (Guindon et al., 2010) to reconstruct the maximum likelihood  
361 phylogenetic tree using the LG substitution model. The tree was visualised with FigTree  
362 v1.4.2 (<http://tree.bio.ed.ac.uk/software/figtree/>).

### 363 Resources

364 The data and Python scripts used to produce the results presented in this manuscript are  
365 available with instructions at (<https://gitlab.com/surajsept/GTvsPT>).

### 366 Acknowledgements

367 The doctoral research of SS in OE's laboratory and research in SK's laboratory is funded by  
368 the Deutsche Forschungsgemeinschaft (DFG) under Germany's Excellence Strategy – EXC  
369 2048/1 – project 390686111.

370 **Author contributions**

371 SS, OE and SK planned and designed the research. SS performed the computational work and  
372 wrote the manuscript with the help of OP, OE and SK.

373 **References**

374 Agerbirk, N., & Olsen, C. E. (2012). Glucosinolate structures in evolution. *Phytochemistry*,  
375 77, 16–45. <https://doi.org/10.1016/j.phytochem.2012.02.005>

376 Agerbirk, N., Olsen, C. E., Heimes, C., Christensen, S., Bak, S., & Hauser, T. P. (2015).  
377 Multiple hydroxyphenethyl glucosinolate isomers and their tandem mass spectrometric  
378 distinction in a geographically structured polymorphism in the crucifer *Barbarea*  
379 *vulgaris*. *Phytochemistry*, 115, 130–142.  
380 <https://doi.org/10.1016/J.PHYTOCHEM.2014.09.003>

381 Benderoth, M., Textor, S., Windsor, A. J., Mitchell-Olds, T., Gershenzon, J., & Kroymann, J.  
382 (2006). Positive selection driving diversification in plant secondary metabolism.  
383 *Proceedings of the National Academy of Sciences of the United States of America*,  
384 103(24), 9118–9123. <https://doi.org/10.1073/pnas.0601738103>

385 Buskov, S., Serra, B., Rosa, E., Sørensen, H., & Sørensen, J. C. (2002). Effects of intact  
386 glucosinolates and products produced from glucosinolates in myrosinase-catalyzed  
387 hydrolysis on the potato cyst nematode (*Globodera rostochiensis* Cv. Woll). *Journal of*  
388 *Agricultural and Food Chemistry*, 50(4), 690–695. Retrieved from  
389 <http://www.ncbi.nlm.nih.gov/pubmed/11829629>

390 Chan, E. K. F., Rowe, H. C., & Kliebenstein, D. J. (2010). Understanding the evolution of  
391 defense metabolites in *Arabidopsis thaliana* using genome-wide association mapping.  
392 *Genetics*, 185(3), 991–1007. <https://doi.org/10.1534/genetics.109.108522>

393 Clarke, D. B. (2010). Glucosinolates, structures and analysis in food. *Analytical Methods*,  
394 2(4), 310. <https://doi.org/10.1039/b9ay00280d>

395 Daxenbichler, M. E., Spencer, G. F., Carlson, D. G., Rose, G. B., Brinker, A. M., & Powell,  
396 R. G. (1991). Glucosinolate composition of seeds from 297 species of wild plants.  
397 *Phytochemistry*, 30(8), 2623–2638.

398 de Kraker, J.-W., & Gershenzon, J. (2011). From amino acid to glucosinolate biosynthesis:  
399 protein sequence changes in the evolution of methylthioalkylmalate synthase in  
400 *Arabidopsis*. *The Plant Cell*, 23(1), 38–53. <https://doi.org/10.1105/tpc.110.079269>

401 DIZ, A. P., MARTÍNEZ-FERNÁNDEZ, M., & ROLÁN-ALVAREZ, E. (2012). Proteomics  
402 in evolutionary ecology: linking the genotype with the phenotype. *Molecular Ecology*,

403 21(5), 1060–1080. <https://doi.org/10.1111/j.1365-294X.2011.05426.x>

404 Douglas Grubb, C., Zipp, B. J., Ludwig-Müller, J., Masuno, M. N., Molinski, T. F., & Abel,  
405 S. (2004). Arabidopsis glucosyltransferase UGT74B1 functions in glucosinolate  
406 biosynthesis and auxin homeostasis. *The Plant Journal*, 40(6), 893–908.

407 Fahey, J. W., Zalcmann, a T., & Talalay, P. (2001). The chemical diversity and distribution  
408 of glucosinolates and isothiocyanates amoung plants. *Phytochemistry*, 56, 5–51.

409 Fisher, R. A. (1930). GENETICAL THEORY OF NATURAL SELECTION. Retrieved from  
410 <http://14.139.56.90/bitstream/1/2033620/1/IVRI%203205.pdf>

411 Gabrys, B., & Tjallingii, W. F. (2002). The role of sinigrin in host plant recognition by aphids  
412 during initial plant penetration. *Entomologia Experimentalis et Applicata*, 104(1), 89–  
413 93. <https://doi.org/10.1046/j.1570-7458.2002.00994.x>

414 Gigolashvili, T., Yatusevich, R., Rollwitz, I., Humphry, M., Gershenson, J., & Flügge, U.-I.  
415 (2009). The plastidic bile acid transporter 5 is required for the biosynthesis of  
416 methionine-derived glucosinolates in *Arabidopsis thaliana*. *The Plant Cell*, 21(6), 1813–  
417 1829. <https://doi.org/10.1105/tpc.109.066399>

418 Guindon, S., Dufayard, J.-F., Lefort, V., Anisimova, M., Hordijk, W., & Gascuel, O. (2010).  
419 New algorithms and methods to estimate maximum-likelihood phylogenies: assessing  
420 the performance of PhyML 3.0. *Systematic Biology*, 59(3), 307–321.

421 Halkier, B. A., & Gershenson, J. (2006). BIOLOGY AND BIOCHEMISTRY OF  
422 GLUCOSINOLATES. *Annual Review of Plant Biology*, 57(1), 303–333.  
423 <https://doi.org/10.1146/annurev.arplant.57.032905.105228>

424 Hamming, R. W. (1950). Error detecting and error correcting codes. *Bell Labs Technical  
425 Journal*, 29(2), 147–160.

426 He, Y., Galant, A., Pang, Q., Strul, J. M., Balogun, S. F., Jez, J. M., & Chen, S. (2011).  
427 Structural and functional evolution of isopropylmalate dehydrogenases in the leucine  
428 and glucosinolate pathways of *Arabidopsis thaliana*. *Journal of Biological Chemistry*,  
429 286(33), 28794–28801. <https://doi.org/10.1074/jbc.M111.262519>

430 Jorge, C., Becker, C., Bemm, F., Bergelson, J., Borgwardt, K. M., Cao, J., ... Zhou, X.  
431 (2016). 1,135 Genomes Reveal the Global Pattern of Polymorphism in *Arabidopsis*  
432 *thaliana*. *Cell*, 166(2), 481–491. <https://doi.org/10.1016/j.cell.2016.05.063>

433 Katoh, K., & Standley, D. M. (2013). MAFFT Multiple Sequence Alignment Software  
434 Version 7: Improvements in Performance and Usability. *Molecular Biology and*  
435 *Evolution*, 30(4), 772–780. <https://doi.org/10.1093/molbev/mst010>

436 Keurentjes, J. J. B., Fu, J., de Vos, C. H. R., Lommen, A., Hall, R. D., Bino, R. J., ...  
437 Koornneef, M. (2006). The genetics of plant metabolism. *Nature Genetics*, 38(7), 842–  
438 849. <https://doi.org/10.1038/ng1815>

439 Kliebenstein, D. J., Kroymann, J., Brown, P., Figuth, A., Pedersen, D., Gershenson, J., &  
440 Mitchell-Olds, T. (2001). Genetic control of natural variation in Arabidopsis  
441 glucosinolate accumulation. *Plant Physiology*, 126(2), 811–825.  
442 <https://doi.org/10.1104/pp.126.2.811>

443 Kliebenstein, D. J., Lambrix, V. M., Reichelt, M., Gershenson, J., & Mitchell-Olds, T.  
444 (2001). Gene Duplication in the Diversification of Secondary Metabolism: Tandem 2-  
445 Oxoglutarate-Dependent Dioxygenases Control Glucosinolate Biosynthesis in  
446 Arabidopsis. *THE PLANT CELL ONLINE*, 13(3), 681–693.  
447 <https://doi.org/10.1105/tpc.13.3.681>

448 Koornneef, M., Alonso-Blanco, C., & Vreugdenhil, D. (2004). NATURALLY OCCURRING  
449 GENETIC VARIATION IN ARABIDOPSIS THALIANA. *Annual Review of Plant*  
450 *Biology*, 55(1), 141–172. <https://doi.org/10.1146/annurev.arplant.55.031903.141605>

451 Kroymann, J., Donnerhacke, S., Schnabelrauch, D., & Mitchell-Olds, T. (2003). Evolutionary  
452 dynamics of an Arabidopsis insect resistance quantitative trait locus. *Proceedings of the*  
453 *National Academy of Sciences of the United States of America*, 100 Suppl(Supplement  
454 2), 14587–14592. <https://doi.org/10.1073/pnas.1734046100>

455 Kroymann, J., Textor, S., Tokuhisa, J. G., Falk, K. L., Bartram, S., Gershenson, J., &  
456 Mitchell-Olds, T. (2001). A gene controlling variation in Arabidopsis glucosinolate  
457 composition is part of the methionine chain elongation pathway. *Plant Physiology*,  
458 127(3), 1077–1088. <https://doi.org/10.1104/pp.010416>

459 Kumar, R., Lee, S. G., Augustine, R., Reichelt, M., Vassão, D. G., Palavalli, M. H., ... Bisht,  
460 N. C. (2019). Molecular Basis of the Evolution of Methylthioalkylmalate Synthase and  
461 the Diversity of Methionine-Derived Glucosinolates. *The Plant Cell*, 31(7), 1633–1647.  
462 <https://doi.org/10.1105/tpc.19.00046>

463 LASKY, J. R., DES MARAIS, D. L., MCKAY, J. K., RICHARDS, J. H., JUENGER, T. E.,  
464 & KEITT, T. H. (2012). Characterizing genomic variation of *Arabidopsis thaliana*: the  
465 roles of geography and climate. *Molecular Ecology*, 21(22), 5512–5529.  
466 <https://doi.org/10.1111/j.1365-294X.2012.05709.x>

467 Lazzeri, L., Curto, G., Leoni, O., & Dallavalle, E. (2004). Effects of Glucosinolates and Their  
468 Enzymatic Hydrolysis Products via Myrosinase on the Root-knot Nematode  
469 *Meloidogyne incognita* (Kofoed et White) Chitw. *Journal of Agricultural and Food  
470 Chemistry*, 52(22), 6703–6707. <https://doi.org/10.1021/jf030776u>

471 Lynch, M., Walsh, B., & others. (1998). *Genetics and analysis of quantitative traits* (Vol. 1).  
472 Sinauer Sunderland, MA.

473 Magrath, R., Banot, F., Morgner, M., Parkin, I., Sharpe, A., Lister, C., ... Mithen, A. A.  
474 (1994). Genetical Society of Great Britain Genetics of aliphatic glucosinolates. I. Side  
475 chain elongation in *Brassica napus* and *A rabidopsis thaliana*. *Heredity*, 72, 290–299.  
476 Retrieved from [https://www.jic.ac.uk/staff/caroline-dean/pdf\\_files/88\\_Magrath\\_R\\_et\\_al\\_1994\\_Heredity.pdf](https://www.jic.ac.uk/staff/caroline-dean/pdf_files/88_Magrath_R_et_al_1994_Heredity.pdf)

478 Marchler-Bauer, A., Derbyshire, M. K., Gonzales, N. R., Lu, S., Chitsaz, F., Geer, L. Y., ...  
479 Bryant, S. H. (2015). CDD: NCBI's conserved domain database. *Nucleic Acids  
480 Research*, 43(Database issue), D222. <https://doi.org/10.1093/NAR/GKU1221>

481 Mewis, I., Ulrich, C., & Schnitzler, W. H. (2002). The role of glucosinolates and their  
482 hydrolysis products in oviposition and host-plant finding by cabbage webworm, *Hellula  
483 undalis*. *Entomologia Experimentalis et Applicata*, 105(2), 129–139.  
484 <https://doi.org/10.1046/j.1570-7458.2002.01041.x>

485 Mikkelsen, M. D., Naur, P., & Halkier, B. A. (2004). *Arabidopsis* mutants in the C–S lyase  
486 of glucosinolate biosynthesis establish a critical role for indole-3-acetaldoxime in auxin  
487 homeostasis. *The Plant Journal*, 37(5), 770–777.

488 Miles, C. I., Campo, M. L. del, & Renwick, J. A. A. (2005). Behavioral and chemosensory  
489 responses to a host recognition cue by larvae of *Pieris rapae*. *Journal of Comparative  
490 Physiology A*, 191(2), 147–155. <https://doi.org/10.1007/s00359-004-0580-x>

491 Mitchell-Olds, T., & Schmitt, J. (2006). Genetic mechanisms and evolutionary significance  
492 of natural variation in *Arabidopsis*. *Nature*, 441(7096), 947–952.

493 <https://doi.org/10.1038/nature04878>

494 Noret, N., Meerts, P., Tolrà, R., Poschenrieder, C., Barceló, J., & Escarre, J. (2005).  
495 Palatability of *Thlaspi caerulescens* for snails: influence of zinc and glucosinolates. *New*  
496 *Phytologist*, 165(3), 763–772. <https://doi.org/10.1111/j.1469-8137.2004.01286.x>

497 Owen, C., Patron, N. J., Huang, A., & Osbourn, A. (2017). Harnessing plant metabolic  
498 diversity. *Current Opinion in Chemical Biology*, 40, 24–30.  
499 <https://doi.org/10.1016/j.cbpa.2017.04.015>

500 Petersen, A., Hansen, L. G., Mirza, N., Crocoll, C., Mirza, O., & Halkier, B. A. (2019).  
501 Changing substrate specificity and iteration of amino acid chain elongation in  
502 glucosinolate biosynthesis through targeted mutagenesis of *Arabidopsis*  
503 methylthioalkylmalate synthase 1. *Bioscience Reports*, 39(7).  
504 <https://doi.org/10.1042/BSR20190446>

505 Pigliucci, M. (2010). Genotype–phenotype mapping and the end of the ‘genes as blueprint’  
506 metaphor. *Philosophical Transactions of the Royal Society B: Biological Sciences*,  
507 365(1540), 557–566. <https://doi.org/10.1098/rstb.2009.0241>

508 Rodman, J. E. (1980). Population variation and hybridization in sea-rocket (Cakile,  
509 Cruciferae): seed glucosinolate characters. *American Journal of Botany*, 1145–1159.

510 Sauter, M., Moffatt, B., Saechao, M. C. C., Hell, R., & Wirtz, M. (2013). Methionine salvage  
511 and S-adenosylmethionine: essential links between sulfur, ethylene and polyamine  
512 biosynthesis. *Biochemical Journal*, 451(2), 145–154.  
513 <https://doi.org/10.1042/BJ20121744>

514 Sawada, Y., Kuwahara, A., Nagano, M., Narisawa, T., Sakata, A., Saito, K., & Yokota Hirai,  
515 M. (2009). Omics-based approaches to methionine side chain elongation in *Arabidopsis*:  
516 characterization of the genes encoding methylthioalkylmalate isomerase and  
517 methylthioalkylmalate dehydrogenase. *Plant and Cell Physiology*, 50(7), 1181–1190.

518 Shannon, C. E. (1948). A Mathematical Theory of Communication. *Bell System Technical*  
519 *Journal*, 27(3), 379–423. <https://doi.org/10.1002/j.1538-7305.1948.tb01338.x>

520 Sharma, S. (2018). Mathematical models of glucosinolate metabolism in plants. Retrieved  
521 from <https://docserv.uni-duesseldorf.de/servlets/DocumentServlet?id=46153>

522 Sønderby, I. E., Geu-Flores, F., & Halkier, B. a. (2010). Biosynthesis of glucosinolates - gene

523 discovery and beyond. *Trends in Plant Science*, 15(5), 283–290.

524 <https://doi.org/10.1016/j.tplants.2010.02.005>

525 Textor, S., Bartram, S., Kroymann, J. J. J., Falk, K. L., Hick, A., Pickett, J. a., & Gershenzon,  
526 J. (2004). Biosynthesis of methionine-derived glucosinolates in *Arabidopsis thaliana*:  
527 recombinant expression and characterization of methylthioalkylmalate synthase, the  
528 condensing enzyme of the chain-elongation cycle. *Planta*, 218(6), 1026–1035.  
529 <https://doi.org/10.1007/s00425-003-1184-3>

530 Textor, S., de Kraker, J.-W., Hause, B., Gershenzon, J., & Tokuhisa, J. G. (2007). MAM3  
531 catalyzes the formation of all aliphatic glucosinolate chain lengths in *Arabidopsis*. *Plant  
532 Physiology*, 144(1), 60–71. <https://doi.org/10.1104/pp.106.091579>

533 Traka, M., & Mithen, R. (2009). Glucosinolates, isothiocyanates and human health.  
534 *Phytochemistry Reviews*, 8(1), 269–282. <https://doi.org/10.1007/s11101-008-9103-7>

535 Weckwerth, W., Wenzel, K., & Fiehn, O. (2004). Process for the integrated extraction,  
536 identification and quantification of metabolites, proteins and RNA to reveal their co-  
537 regulation in biochemical networks. *PROTEOMICS*, 4(1), 78–83.  
538 <https://doi.org/10.1002/pmic.200200500>

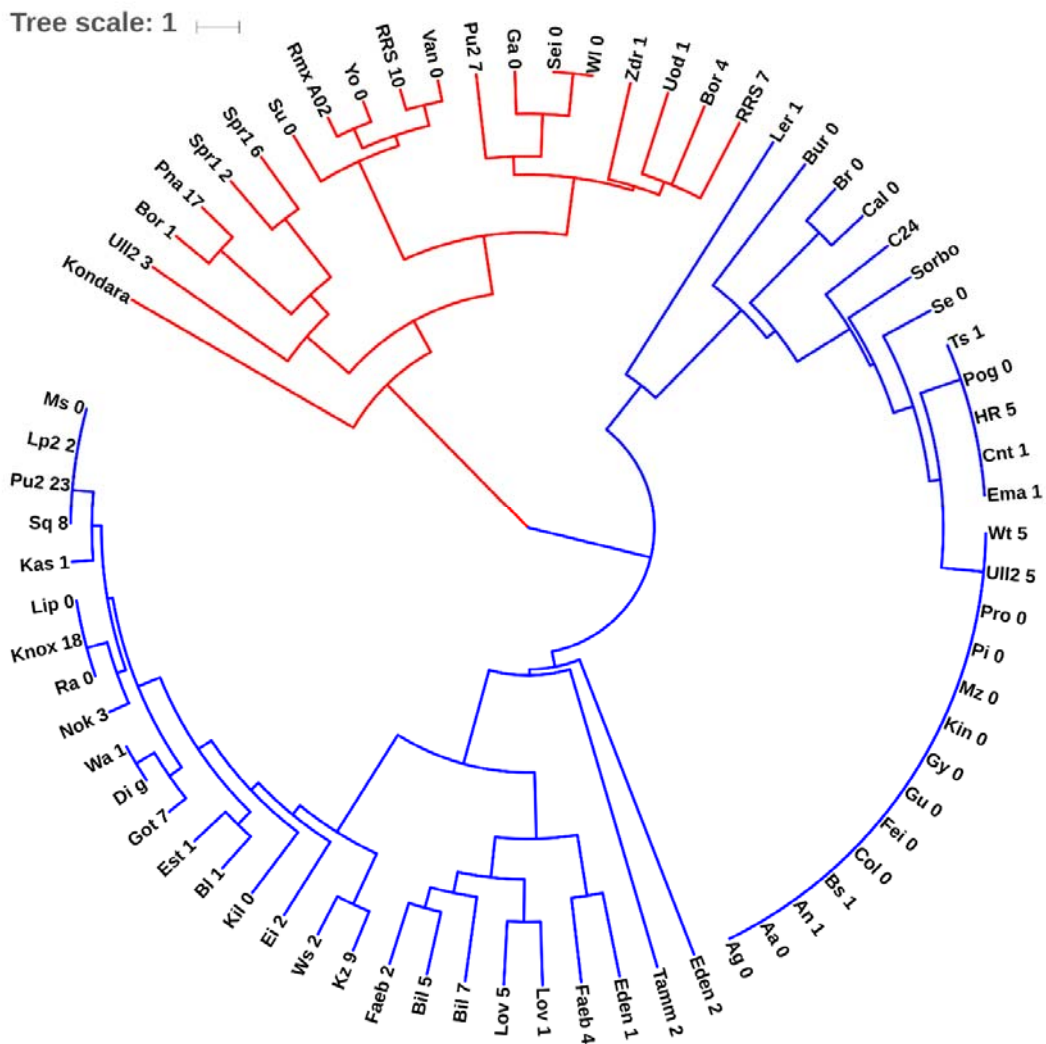
539 Wittstock, U., Agerbirk, N., Stauber, E. J., Olsen, C. E., Hippler, M., Mitchell-Olds, T., ...  
540 Vogel, H. (2004). Successful herbivore attack due to metabolic diversion of a plant  
541 chemical defense. *Proceedings of the National Academy of Sciences*, 101(14), 4859–  
542 4864. <https://doi.org/10.1073/pnas.0308007101>

543

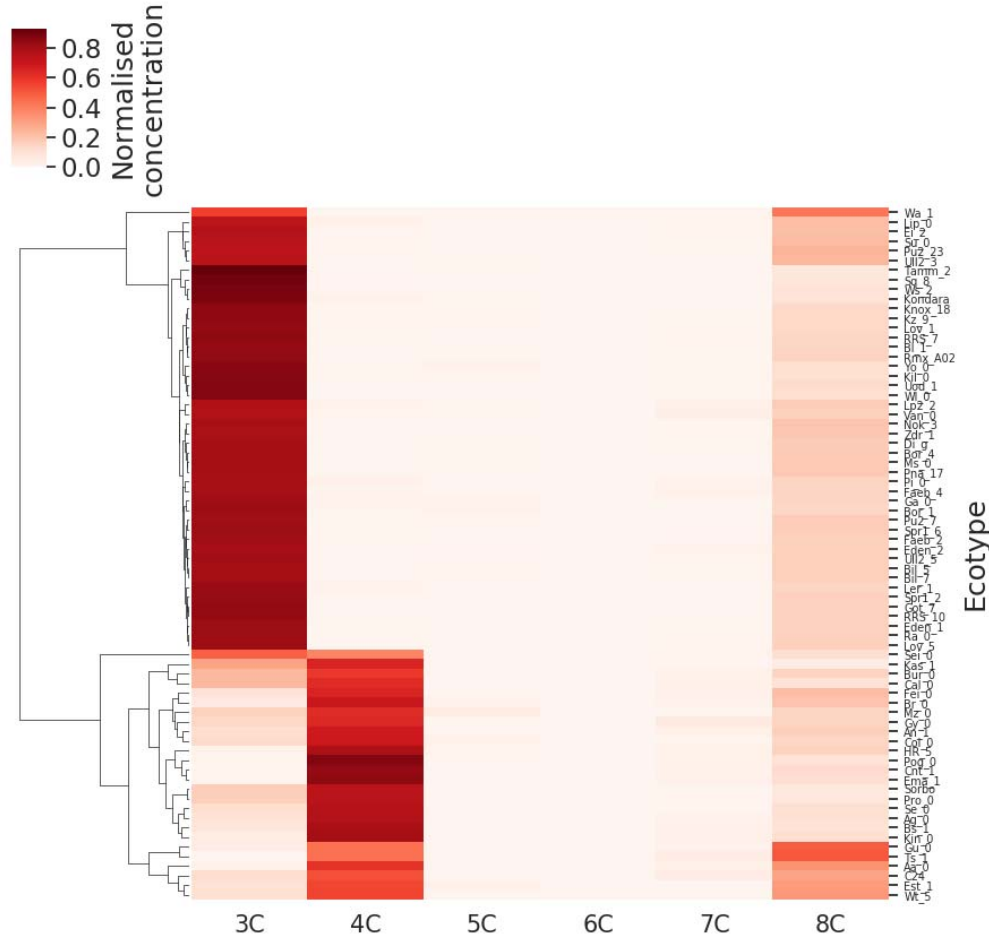
544

545 **Figures**

546 *Figure 1: Mid-point rooted phylogenetic tree showing the evolutionary relationship among coding regions of annotated*  
547 *MAMI gene of 72 *Arabidopsis thaliana* ecotypes. The red branch represents ecotypes showing higher similarity to the*  
548 *MAM2 sequence. The scale bar is substitutions per position.*



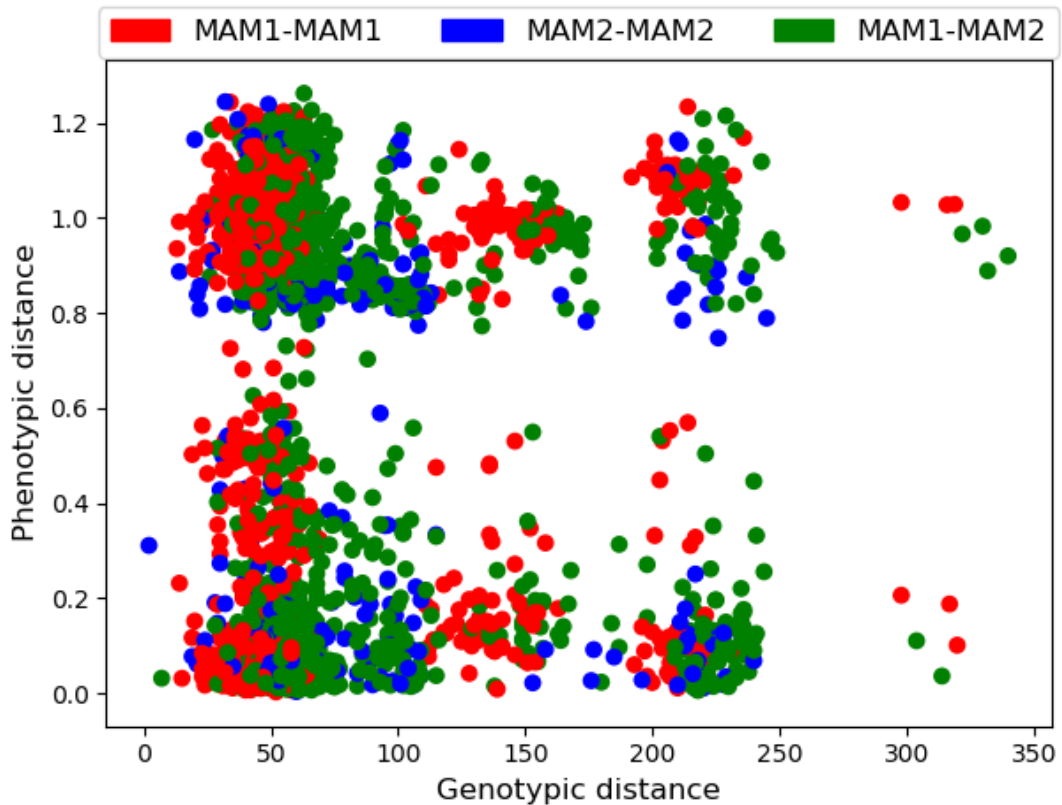
552 *Figure 2: Clustered heatmap of the GSL composition across 72 different *A. thaliana* ecotypes. The top cluster is composed of*  
 553 *ecotypes having high concentration of 3C GSLs, the lower cluster corresponds to the ecotypes accumulating high*  
 554 *concentrations of 4C GSLs.*



555

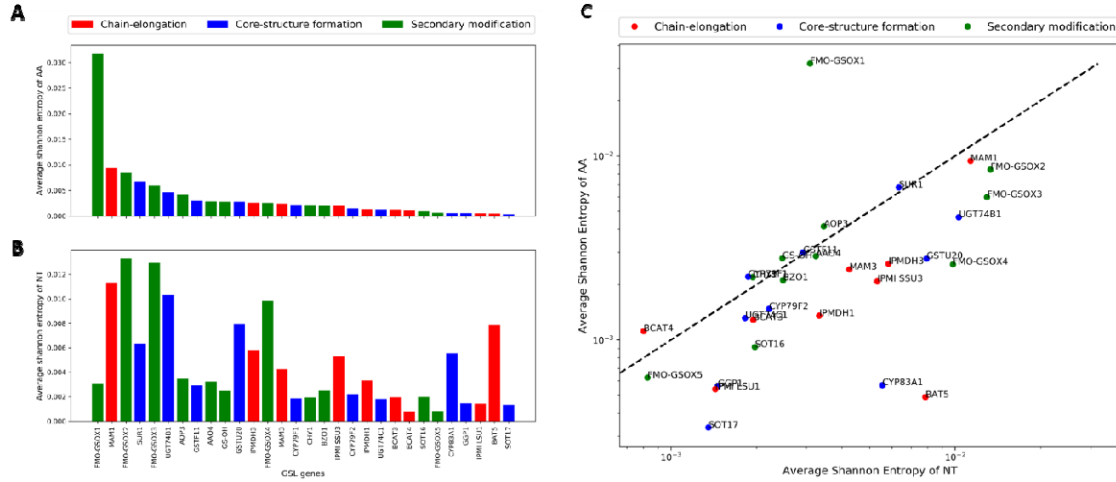
556

557     *Figure 3: The genotypic versus phenotypic distance. Every ecotype is assigned to possess either MAM1 or MAM2, based on*  
558     *the sequence similarity of annotated MAM1 gene. Each dot represents a pair of ecotypes. The colours red and blue denote*  
559     *pairs, where both ecotypes show high similarity to the coding region of MAM1 and MAM2 sequence, respectively, the green*  
560     *dots denote heterogeneous pairs.*



561  
562

563 *Figure 4: Diversity of GSL genes from 72 *A. thaliana* ecotypes. (A) The bars represent the diversity of the amino-acid (AA)  
564 residues of respective GSL genes. The bars are colour coded to denote genes from the chain-elongation process, core-  
565 structure formation and secondary chain modifications by red, blue and green colours, respectively. (B) The bars represent  
566 the diversity of the nucleotides (NT) of respective genes. The bars are colour coded as in (A). (C) Diversity of NT residues  
567 plotted against the diversity of AA residues of respective GSL genes. Each dot is colour coded to denote genes as in (A) and  
568 (B). The black dashed line is a linear regression line.*



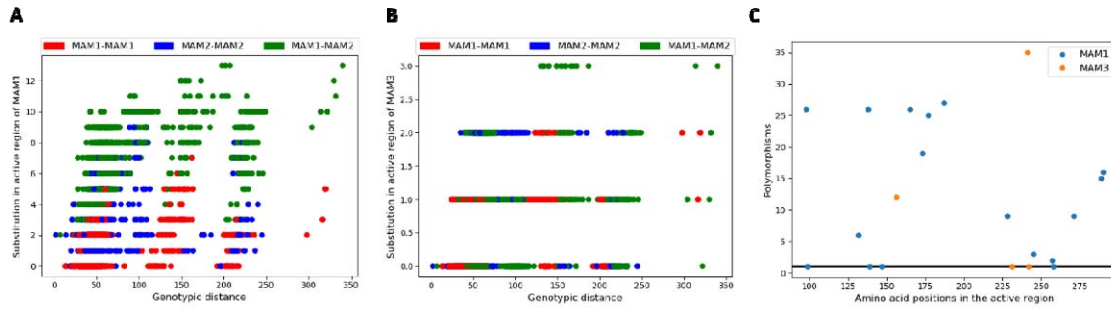
569  
570

571

572

573

574 *Figure 5: Polymorphisms in the active region of MAM synthases. (A) Substitutions in the active sites of MAM1 versus the  
575 Genotypic distances. (B) Substitutions in the active sites of MAM1 versus the Genotypic distances. (C) Polymorphisms in the  
576 active region of MAM1 and MAM3.*



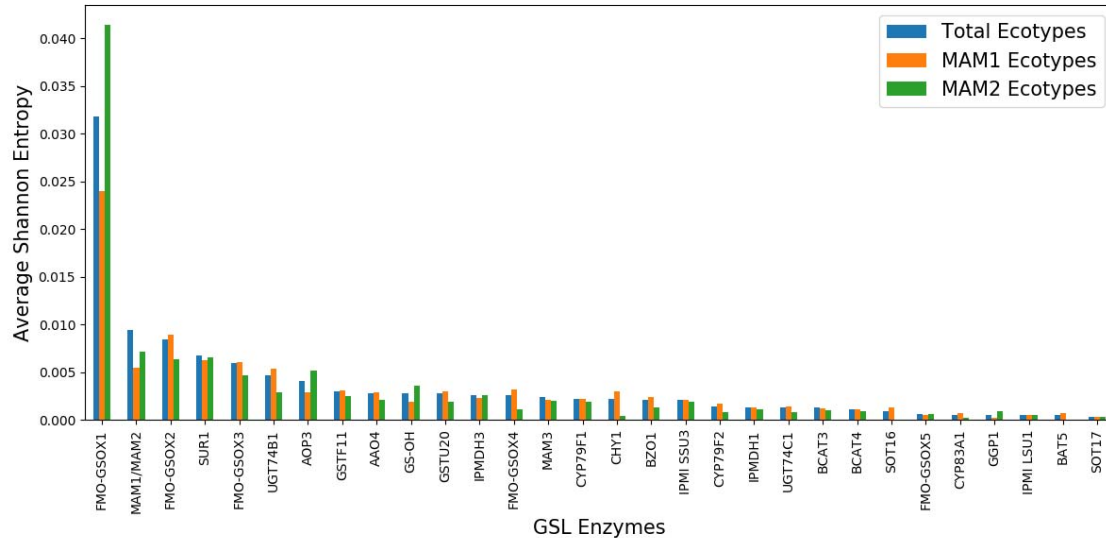
577

578

579

580 **Supplementary Figures:**

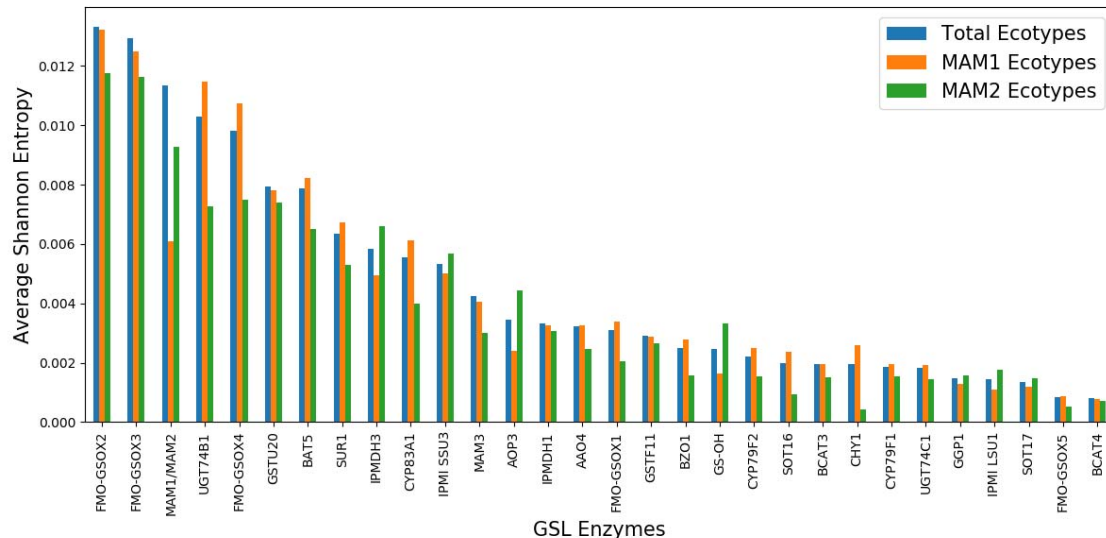
581 *Figure 1: Diversity of GSL enzymes from different ecotype subgroups. The bars represent the diversity of the amino-acid*  
582 *residues of respective GSL genes. The blue bars denote all 72 ecotypes, while orange and green denote ecotypes having*  
583 *MAM1 and MAM2, respectively.*



584

585

586 *Figure 2: Diversity of GSL enzymes from different subgroups of ecotypes. The bars represent the diversity of nucleotide*  
587 *sequences of respective GSL genes. Colour coding is same as Supplementary Figure 1.*



588